Review

Journal of the Brazilian Chemical Society

https://dx.doi.org/10.21577/0103-5053.20240119

J. Braz. Chem. Soc. **2024**, *35*, 10, e-20240119, 1-15

Status and Prospects of Molecular Simulations for Drug Discovery

Hugo Verli [*,a,b] ***and Chris Oostenbrink*** [c,d]

[a]*Programa de Pós-Graduação em Biologia Celular e Molecular, Centro de Biotecnologia, Universidade Federal do Rio Grande do Sul, 90650-001 Porto Alegre-RS, Brazil*

[b]*Instituto Nacional de Ciência e Tecnologia em Biologia do Câncer Infantil e Oncologia Pediátrica (INCT BioOncoPed), 90035-003 Porto Alegre-RS, Brazil*

[c]*Department of Material Sciences and Process Engineering, Institute of Molecular Modeling and Simulation, University of Natural Resources and Life Sciences, Vienna, Muthgasse 18, 1190 Vienna, Austria*

[d]*Christian Doppler Laboratory for Molecular Informatics in the Biosciences, University of Natural Resources and Life Sciences, Vienna, Muthgasse 18, 1190 Vienna, Austria*

During the past 30 years, molecular simulations (MS) have become increasingly popular among medicinal chemists, being recognized as a promising tool to reduce drug development costs and timelines while increasing its success. From the refinement of docking experiments during the 1990's to the contemporary possibility to produce accurate models of ligand intrinsic activity and affinity, the use of simulations in medicinal chemistry has progressed rapidly, becoming an essential tool in modern drug discovery pipelines. However, in spite of their potential, *in silico* methods and MS have historically been dependent on a tradeoff between computational cost and accuracy, which not uncommonly limits their impacts on drug development. In this context, this review presents a concise and up-to-date summary of the role of MS in medicinal chemistry, and examines its participation in recent advancements of both ligand-based and structure-based drug discovery, free-energy predictions, and model accuracies. In addition to offering a synopsis of the potential benefits of MS on drug discovery, this review intends to aid users to both understand the limitations of computational methods and to design more accurate experiments that, as a consequence, will have an increasing impact on the development of new therapeutics.

Keywords: drug design, molecular simulations, free energy, equilibration, simulation length, data accuracy

1. Introduction

The recognition of molecular flexibility was epochal. The concept of conformation as currently understood can be traced[1] to Haworth, in his seminal book *The Constitution of Sugars*,[2] published in 1929. However, it was not until the beginning of the 1960's that the understanding of molecular flexibility matured to encompass protein dynamics, taking as a hallmark the studies of protein folding by Anfinsen *et al.*[3] The 1960's also saw the first reports of software capable of manipulating protein structures by using oscilloscopes.[4] And, since the 1970's, with the work from Nobel laureates Levitt and Warshel[5] and the seminal work of McCammon *et al.*,[6] the simulation of biomolecular dynamics became a reality within the scientific community.

In the context of drug discovery, the structural basis of ligand-receptor recognition took about 50 years to evolve from a mechanical concept offered by the "Lock and Key" model from Emil Fischer, developed in the end of the nineteenth century, to the dynamic description of enzyme-substrate recognition from Koshland[7] (i.e., new conformational states, not previously observed in solution, emerge upon complexation) and to the thermodynamic understanding of the process of conformational selection (i.e., molecules exist in an ensemble of different conformations and the partners select each other based on complementarity).[8] Since then, "Induced Fit" or

*e-mail: hugoverli@gmail.com
Editor handled this article: Carlos Maurício R. de Sant'Anna (Guest)

"Conformational Selection" models can be applied to drug-receptor modulation in general, as in allosterism and agonism, which are currently well established by a plethora of experimental techniques that include X-ray crystallography, nuclear magnetic resonance (NMR), circular dichroism, infrared spectroscopy, fluorescence, cryoelectron microscopy, and many others. More recently, the importance of the time during which a drug remains physically bound to its target receptor, that is, its residence time, has been recognized,[9] greatly expanding the timescale required to represent the pharmacologic action of drugs.

With the emergence and continuous development of *in silico* simulation techniques focused on organic drug-like compounds, the scientific community has produced progressively more accurate computational models of drug action, allowing researchers to not only refine and complement empirical results but also, within certain parameters, to circumvent some experimental limitations and reduce the cost and time required to obtain results in comparison to empiric non-computational techniques ("computational experiments" are for simplification usually called "computational data." The word "experiment" is commonly retained for benchwork-related data, or "wet science." However, the concept that *in silico* results, by its theoretical nature, are of lower quality than results obtained by experiments that do not use computer models, is obsolete. All types of experiments, either computational or empirical, have limitations and advantages. In fact, it is increasingly difficult to find experiments that do not require any form of computational modeling). In fact, the potential of *in silico* experiments has increased acutely in recent decades (Figure 1), following a steady increase in computational power, software optimization, and methodologic development that have progressively transferred its bottleneck from infrastructure (hardware and software) to experimental design and data analysis. Numerous compounds developed through computational methods[10] have entered clinical trials leading to drug approvals, from the use of comparative modeling on the development of captopril and zanezepil,[11] to the design of novel human immunodeficiency virus (HIV) protease inhibitors as lopinavir based on analyses of its interactions with mutant residues[11] and the use of fragment based drug discovery for the identification of vemurafenib.[12] In fact, it is implausible that the development of new drugs do not include, at some point, computational tools, as in the identification of genes, the screen of molecular libraries or the application of structure-based drug design methods.[10] Additionally, the emergence of machine learning and artificial intelligence models may be heralding a "golden age" of computational drug discovery that, on the other hand, may suffer from a "point and click" use of complex tools without concern for methodological characteristics, best practices, and limitations. In this sense, the accuracy of computational simulations remains highly dependent on user expertise, on how the simulations are prepared, and on how results are interpreted. In this context, the current review intends to present some of the main advancements of computational simulation over the past decades, their major potentials and limitations, as well as some methodological best practices, with the aim to aid medicinal chemists to produce more accurate models for their drug discovery pipelines while wasting less time following false leads based on methodological limitations.

Therefore, this work will begin by discussing methodological approaches to the computational assessment of molecular flexibility, followed by a description of the potential impacts of molecular simulations (MS) on ligand-based drug discovery (LBDD) and structure-based drug discovery (SBDD), ending with considerations regarding future prospects on the field.

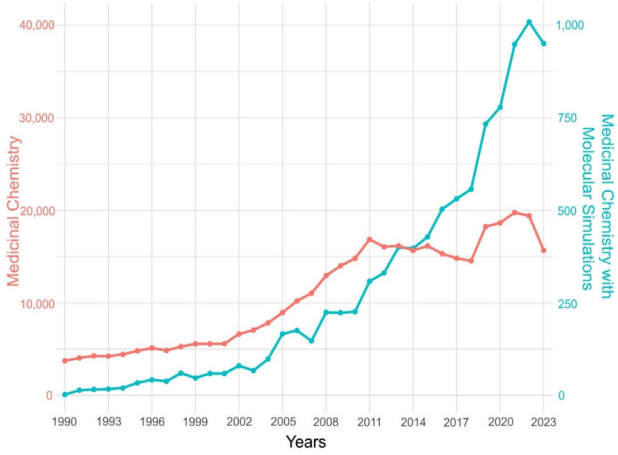

Figure 1. Publication count *per* year, produced from data obtained from Web of Science (WoS). Searches were performed using keywords: (red) "chemistry, medicinal," a category from WoS (left y axis), (blue) and its combination with the keywords "molecular simulation" or "molecular dynamic" or "metadynamics" or "umbrella sampling" (right y axis). Access date 05/12/2023. The steepness of the increase in molecular simulations on drug discovery publications in the last 10 years demonstrate the popularization of these techniques on the field.

2. Accessing Molecules Flexibility

2.1. Representation of drug-like compounds

The computational representation of drug-like compounds at the atomistic level is performed primarily by using quantum mechanics (QM), molecular mechanics (MM), a combination of these methods (QM/MM) and, more recently, through machine learning potentials trained from QM data (coarse-grained methods are

theoretically able to describe drug-like compounds, but are impaired by the challenge of parameterizing drugs chemical landscape, so they will not be discussed here). QM methods usually describe molecular properties more accurately, but incur a higher computational cost and it can be challenging to find the proper method, functional or basis set for your specific system. The MM approach, in turn, allows simulations of molecular systems beyond 10^6 atoms, but requires a careful calibration of energy functions to empirical data to properly describe molecules (i.e., the force field). Although this parameterization is well established for biomacromolecules (as in AMBER,[13] CHARMM,[14] GROMOS,[15] and OPLS)[16] as based on known and repetitive building blocks (e.g., amino acid residues, nucleotides, lipids and monosaccharides), drug-like compounds impose challenges due to their structural diversity. Because the quality of these parameters is central to the accuracy of computational models, several potential solutions to this problem have been explored in the past decades and so avoid (at some level) the extra parameterization effort by the user.

From the pioneering work of Hendrickson[17] in the 1960's to a series of force field developments by Allinger and co-workers[18,19] between the 1970's and 1990's, the development of MMFF94 by Halgren[20] is notable, and likely the first force-field development focused on drug discovery. Even after 30 years, Halgren's work is still relevant, as exemplified by its role in assisting the high accuracy of the DockThor[21] engine. However, these initial developments of force fields for organic drug-like compounds were not associated to the parameters necessary to describe the dynamics of biomolecules, particularly those of proteins, thus impairing MS of ligand-receptor complexes obtained by using MMFF94. This limitation was tackled by AMBER GAFF,[22] CGEnFF[23,24] and CHARMM-GUI[25] and, for GROMOS, in the initial approach by PRODRG,[26] and later more accurately by ATB[27] (see Table 1 for a comprehensive list of simulation packages, force fields and topology builders for drug-like compounds; check also the literature[36] for further information on simulation engines trends). Nonetheless, all solutions indicated above share an intrinsic limitation of parameterization due to the difficulty of anticipating chemical diversity. Consequently, the user should be conscious of the possible lack of accurate parameters for uncommon functional groups and atoms, and should be aware of the absence of appropriate torsional terms in the force field database, which could impact the accuracy of the ligand-receptor interactions described in MS. In addition, the proper selection of protonation or tautomeric states for the potential bioactive compounds under study may also have a strong influence on the obtained interaction energies (e.g., hydrogen bonds *versus* salt bridges) and, therefore, on how conformational events propagate through the target receptor. This also applies for the receptor, particularly in the case of histidine residues, that can occur in different protonation states in physiological pH. Even with the use of tools to predict pK_a values for the residues side chains, an analysis of the residues that interact with a histidine may aid to identify the ionization state likely to occur physiologically and, as a consequence, to be employed on the simulations. The combination of inadequate parameters and bad ligand preparation may give origin to errors as inaccurate ligand conformations, may impair the ability of simulations to properly represent conformational activation of target receptors by bioactive compounds or even induce the dissociation of the ligand-receptor complex. In other words, these errors could be of: (*i*) structural/conformational nature, that could be limited on tight binding clefts (where the ligand cannot move) or highly flexible ensembles (where the ligand moves so much that it creates some conformational "noise"), or (*ii*) energetic nature, that could greatly interfere in free-energy predictions, being likely more sensitive to bad parameters than the first case. However, these problems may be less likely in future iterations of automated ligand topology builders due to improved set of parameters, based on larger data sets that will cover a major part of the potential chemical landscape.

In principle, the limitations of force field-based descriptions of drug-like compounds might be circumvented by using hybrid QM/MM methods, bringing the ligand into the QM region, and therefore not requiring previous parameterization. On the other hand, the user should be aware of the employed method (e.g., semi-empirical, *ab initio*, or density functional theory), functionals and basis sets. This choice is intrinsically associated to the chemical structure of the compound under study and how well a specific method describes its properties. Unfortunately, the embedding schemes that describe the interactions between QM and MM regions are far from ideal, ranging from simple mechanical embedding via electrostatic embedding to more advanced polarizable embedding schemes. Furthermore, the inclusion of a QM region in an molecular dynamics (MD) simulation still substantially increases computational cost, seriously limiting the accessible time scale. An alternative approach would be to first sample the compounds of interest on large time scales by using MM, then identify conformational states of interest and refine these states through shorter QM/MM simulations (or even pure QM in some situations, as through MOPAC MOZYME)[37] to describe intermolecular interactions of electronic origin. For instance, one can

Table 1. Most common packages for atomistic unbiased molecular dynamics simulations, including the main force fields included and available tools to produce organic, drug-like topologies

Program	Force field	Ligand topology builder
AMBER[28]	AMBER[a]	Antechamber, CHARMM-GUI, ATB
CHARMM[29]	CHARMM[b], MMFF94	CHARMM-GUI, LigParGen
Desmond[30]	OPLS4[c]	Maestro, CHARMM-GUI, LigParGen
GROMACS[31]	AMBER, CHARMM, GROMOS, OPLS[d]	ACPYPE, ATB, CHARMM-GUI, LigParGen
GROMOS[32]	AMBER, GROMOS[e]	ATB
NAMD[33]	CHARMM, X-PLOR[f]	CHARMM-GUI, LigParGen
OpenMM[34]	AMBER14, CHARMM36, AMOEBA, ANI[g]	OpenMM, CHARMM-GUI, LigParGen
Tinker[35]	AMBER, Allinger MM, OPLS, MMFF94, AMOEBA[h]	Tinker, CHARMM-GUI, LigParGen

[a]Multiple versions, but the recommended ones are ff19SB (proteins), OL21 (deoxyribonucleic acids (DNA)), OL3 (ribonucleic acids (RNA)), GLYCAM_06j (carbohydrates), lipids21 (lipids), gaff2 (organic compounds) and multiple models for water and ions; [b]multiple versions, but the recommended one is CHARMM36, that include parameters for proteins, nucleic acids, lipids, carbohydrates and organic compounds (CGenFF) as well; [c]additional force fields from OPLS, AMBER and CHARMM families are also available; [d]multiple versions of these force fields are available on GROMACS, including AMBER versions 94, 96, 99, 99SB, 99SB-ILDN, 03 and GS; CHARMM versions 19, 22, 27 and 36; GROMOS versions 43a1, 43a2, 45a3, 53a6 and 54a7; and version OPLS-AA/M; [e]the latest versions of GROMOS force field available under GROMOS package are 45A3/4, 53A5/6, 54A7 and 54A8; [f]include versions of force fields present on CHARMM and X-PLOR packages. [g]other force fields are also available on OpenMM, including GLYCAM parameters, CHARMM Polarizable force field and OpenFF or AMBER GAFF for organic compounds; [h]Tinker is able to use multiple version of several force fields, such as Amber (ff94, ff96, ff98, ff99, ff99SB), CHARMM (19, 22, 22/CMAP), Allinger MM (MM2-1991 and MM3-2000), OPLS (OPLS-UA, OPLS-AA) and AMOEBA (2004, 2009, 2013, 2017, 2018), among others.

check with such an approach if a crystallographic ion is indeed coordinated to the enzyme.[38] These limitations due to high computational costs, however, may be overcome in the near future by substantial advancements in machine learning-derived potentials trained on large, high-quality data sets derived from quantum mechanical data, such as ANI (accurate neural network engine for molecular energies) potentials,[39] substituting the QM part and allowing faster calculation.[25]

2.2. MD simulations

Conventional MD simulations have been conducted for almost half a century,[5,6] and have allowed researchers to accurately represent molecular phenomena in solution.[40] MD simulations can represent a molecular system as a function of time while including elements essential to the representation of ligands activity, such as solvent, ions, cofactors, amino acid ionization, membrane chemistry, and ultimately, how these factors entangle in a dynamic system. However, the accuracy of MD-based predictions depends on a series of factors, such as the selected force field, simulation setup, system equilibration, and the extent of the system sampling.[40,41] With the continuous advancement of computational power dictated by Moore's Law and software optimization (particularly of graphic processing units, GPUs), the time scale accessible to medicinal chemists has increased steadily in the last 30 years (Figure 2).

The length of a simulation is one of many factors that may impact a model accuracy. Additionally, the preparation

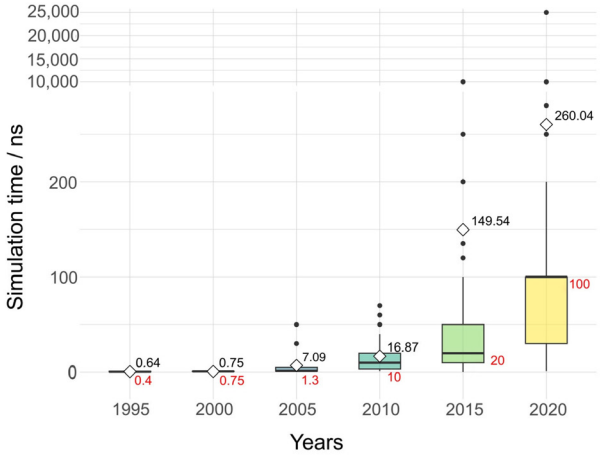

Figure 2. Boxplot of the evolution of MD simulation times associated with drug discovery, in nanoseconds, from 1995 to 2020. Data were collected on the WoS by combining the terms "molecular dynamics" and "drug discovery." Only full papers were considered, resulting in ca. 3,300 articles between 1995 and 2020. Additionally, these papers were curated manually to focus only on conventional MD, resulting in a total of ca. 730 papers from which data were collected. For each paper, only the single longest simulation was considered. The red values present the median values of the simulation lengths, while the black values (with a white diamond) represent the average values. Black circles represent the outliers.

of the system, including the equilibration phase, will contribute to how well a MD simulation will mimic the desired biological conditions. It is usually constituted by an initial equilibration phase, in which the system is gradually heated, or the simulation is progressively freed from positional restraints or, alternatively, a combination of the two approaches. Equilibration is essential to allow solutes to lose the structural memory of

the crystallographic environment (that feature high protein and salt concentrations), while acquiring interactions with solvent molecules. But this simulation step, which is commonly neglected by users, carries a much deeper importance and implication to the success of a MD-based molecular model. The average properties obtained from simulations will only be representative when the equilibration length is longer than the time that a given property requires to reach equilibrium (the property called relaxation time) and when the simulation period is sufficiently longer than the relaxation time of the property of interest.[42] Unfortunately, different properties possess dissimilar relaxation times. Consequently, the equilibration time should be adjusted to the property of interest. For example, physical chemical properties such as the system volume, density, and total/kinetic/potential energies will usually equilibrate in matter of picoseconds, while the protein atom-positional root-mean-square deviation may require nanoseconds to microseconds to achieve equilibrium, or may even fail to equilibrate during the simulation time. In our research group,[43] we use only a relaxation of positional restraints. It simplifies the equilibration by removing the graduate heating, but still allow the solute or ligand-receptor complex to slowly accommodate to the solvent and dissipate crystallographic forces. Usually, our setup includes an initial 1 ns NVT (the number of simulated particles, simulation cell volume and temperature are all kept fixed) simulation with all atoms from the ligand-protein complex restrained by 5,000 kJ mol^{-1}, followed by five NPT (the number of simulated particles, simulation cell pressure and temperature are all kept fixed) simulations, during 1 ns each, with decreasing positional restraints on the complex of 5,000, 4,000, 3,000, 2,000 and 1,000 kJ mol^{-1}, after which the production run initiates. But this setup should be adapted to the system under study. For example, for transmembrane proteins an initial step to equilibrate the membrane should be performed, restraining the protein (and bioactive compound, if present) atomic positions. Such longer and more subtle equilibration protocol could be particularly important in the equilibration of ligand-receptor complexes, where bad contacts between atoms produced by docking or crystallization could impact on binding stability, or when a given protein, such as a G-protein-coupled receptors, GPCRs, shows an activated conformation produced by a ligand, made by a net of delicate interactions that could be lost in abrupt equilibrations.

The simulation length, especially for unbiased MD, represents how much of a given molecule conformational ensemble is sampled by the computational model. Accordingly, simulation length is one of the major aspects that define the accuracy of simulations in representing the behavior of the molecular system under conditions that supposedly mimic native states. Ideally, simulation time scales should be beyond the relaxation times of the phenomena under study,[40] which can range from milliseconds to hours.[44] In this context, the length of simulations used by medicinal chemists started modestly on a picosecond time scale during the 1990's and the first decade of the 2000's, and then increased slowly up to the current decade, when it was boosted by an order of magnitude compared to the previous period, which is a remarkable achievement. Currently, the average time scales of MD simulations applied to drug discovery are on the order of 10^2 ns and are moving towards 10^3 ns. Nonetheless, 75% of MD applications are below the 10^2 ns time scale, which may not capture all relevant processes observed in longer simulations.

In contrast to simulation times (Figure 2), the lengths of equilibration times have shown a very limited evolution over recent decades, remaining between tens to a few hundred picoseconds (Figure 3). While such timescales are usually adequate to equilibrate simulation box conditions, they are far from sufficient for protein equilibration, which in turn will depend on molecular flexibility and size, as well as on the molecular phenomena of interest (e.g., a small globular protein, a multidomain protein, a small or a large loop, a docking pose accommodation, the estimation of ligand half-life of complexation, and allosteric activation of

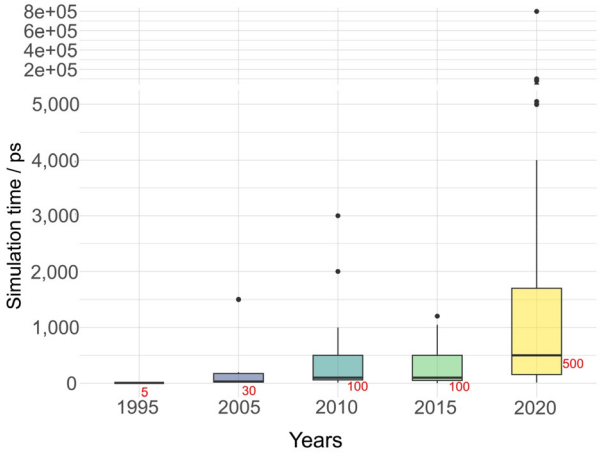

Figure 3. Boxplot of the evolution of equilibration times in preparation of MD simulations associated with drug discovery, in picoseconds, from 1995 to 2020. Data were collected on the WoS, combining the terms "molecular dynamics" and "drug discovery." Only full papers were considered in the analysis, resulting in ca. 3,300 articles. Additionally, these papers were curated manually to focus only on conventional MD, resulting in a total of ca. 730 papers, from which the data were collected. For each paper, only the single longest simulation was considered. Red values present the median values of the simulation lengths, while black values (with a white diamond) represent the average values. Black circles represent outliers. Equilibration schemes included thermalization and progressive relaxation of positional restraints, or a combination of both.

G-protein-coupled receptors, GPCRs). On the other hand, if a hypothetical 100 ns simulation was equilibrated by 100 ps, but only the last 10 ns were analyzed, in practice the system was equilibrated by 90 ns, and not 100 ps. Much more troublesome is that approximately 50% of the reviewed papers from 1995 to 2020 that reported the use of molecular dynamics simulations in medicinal chemistry projects neither equilibrated nor mentioned equilibration of their systems. This omission is even more common when commercial packages are used ("black boxes").

A series of approaches has been developed and integrated into conventional MD to at least partially circumvent the challenges of representing ligand-receptor complexes on biological time scales. For example, techniques as clustering or PCA (principal component analysis) are used to reduce the dimensionality of simulation sampling by removing noise while concentrating the user analysis on main conformational states that are (hopefully) relevant for the biological process under study. On the other hand, an increasingly common approach that is even required as a standard by some journals[45] is the use of replica simulations that start from different velocities or even coordinates (and the combination of these trajectories can be filtered by PCA, for instance). It is important to emphasize that a PCA analysis of multiple replicas of the same system will not be directly comparable, unless the user combine all replica in a single trajectory (as well as control simulations). Later, each state can be comparatively located on the map, as well as its trajectory during simulations. The concept is that each simulation will start from a different point in the free energy landscape of a given molecular system, cover a different path, and ideally converge with a similar sampling, while the properties of interest would be presented as averages among the replica. This approach can robustly increase the sampling of a simulation while allowing the user to focus on reproducible molecular phenomena and to exercise caution when evaluating rare events,[46] particularly when combined to control simulations, that is, a MD of the uncomplexed receptor (as a negative control) or MDs of the receptor complexed to known ligands (as positive controls).

2.3. Enhanced sampling techniques

Alternatively to increase sampling by increasing its length and adding replicas, multiple approaches have been developed to improve simulation sampling. These include local elevation (LE) simulations,[47] metadynamics,[48,49] replica-exchange simulations,[50,51] gaussian accelerated molecular dynamics,[52,53] normal modes,[54,55] normal modes with excited states,[56] umbrella sampling,[57,58] and accelerated enveloping distribution sampling,[59] among many others (see Table 2 for a list of some enhanced sampling techniques and associated packages). Distinguished by either requiring or not requiring a collective variable (a variable, property or path that will guide the sampling, as in LE and metadynamics), these approaches employ different methods to allow simulations to circumvent energy barriers, and thereby sample a larger region of the conformational space associated to a given molecular system. An analysis of these techniques has been previously reviewed.[62] However, the user should consider some issues when employing enhanced sampling techniques (depending on the method), such as: (*i*) high computational cost; (*ii*) subjectivity of the definition of collective variables; (*iii*) observation of high energy conformational states, with no relevance for biological conditions; and (*iv*) the level of complexity associated to the use of the technique of interest. Nevertheless, the role these methods will have on drug discovery will certainly increase in the next years, and in some applications, it will likely be the new standard.

Table 2. List of some of the most common enhanced sampling techniques, as well as the packages where they are currently found

Method	Program
Accelerated Enveloping Distribution Sampling (A-EDS)	GROMOS
Accelerated Weight Histogram (AWH)	GROMACS
Enveloping Distribution Sampling (EDS)	CHARMM, GROMOS
Gaussian Accelerated Molecular Dynamics (GaMD)	AMBER, GROMOS, OpenMM
Local Elevation (LE)	GROMOS
Metadynamics	PLUMED[60]
Normal Modes (NM)	AMBER, CHARMM, GROMACS
Normal Modes with Excited States (MDeNM)	MDexciteR[61]
Potential of Mean Force (PMF)	AMBER, CHARMM, GROMACS, OpenMM, Tinker
Replica-Exchange Molecular Dynamics (REMD)	AMBER, CHARMM, GROMACS, GROMOS, OpenMM
Umbrella Sampling (US)	AMBER, CHARMM, GROMACS, GROMOS, OpenMM

3. Molecular Flexibility Impact on LBDD

With our current understanding of drug activity as a consequence of the modulation of a specific target receptor (or receptors, in the case of multi-target drugs) and the consequent implications for drug development, the analysis of free ligand dynamics using LBDD may seem counterintuitive. So why pay attention to uncomplexed ligand conformation?

The first and likely most obvious reason is that receptors' 3D structures may not always be available from either experimental (e.g., NMR, X-ray crystallography, and cryoelectron microscopy) or computational approaches (primarily through AlphaFold,[63] because of the great advancement and publicity that AlphaFold brought, some researchers[64] may believe that it can predict high fidelity models for all proteins. This is not true. It certainly can predict excellent models for an extremely large number of proteins, but the user should be aware of the quality statistics offered with AlphaFold results. Global or local problems are far from uncommon with these models, and should be taken carefully into consideration) whereas other tools such as Rosetta and Swiss Model remain important for specific applications).[65,66] In such situations, traditional approaches to building structure-activity relationships (SAR) from ligands and produce predictive models of the bioactivity of a series of congeners will remain relevant to medicinal chemistry in the foreseeable future (Figure 4). Because the user may not know the ligand's bioactive conformation, and since such conformation may not necessarily correspond to a minimum energy state, tools were developed in the past decades to perform fast conformational analyses and to produce representations of the conformational diversity of drug-like compounds,[70] including recent deep learning based approaches.[71] However, the use of such tools is limited by their potential prediction of conformations that are not observed under biological conditions or that represent high energy states. As an alternative to the identification of single conformational states for SAR/QSAR (quantitative structure-activity relationships) studies, the consideration of the ensemble as a dimension to be explored in QSAR approaches was pioneered by Hopfinger[69] in the late 1990's and remains a relevant tool for medicinal chemists.[72] Not only an alternative approach for QSAR modelling, Hopfinger's 4D-QSAR accelerated the recognition that pharmacophoric models are not static entities, but snapshots of a dynamic network of probabilistic intermolecular interactions, whereas the idea of an ensemble space was already proposed in the 1980's[73] (Figure 4). As a consequence, the idea of a bioactive conformation may be understood as a set of similar conformational states from a bioactive compound able to promote similar responses by the target receptor.

As an alternative to the generation of ligand conformational diversity, MD simulations can produce accurate representations of conformational states accessible in simulated solutions using water or organic solvents, being limited primarily by force field accuracy.[74] Drug-like compounds, due to their small size, are simulated quickly and possess smaller conformational landscapes compared to proteins; consequently, robust sampling should be accessible for compound series used to produce SAR or QSAR models. While this strategy to generate conformational diversity will not enable the anticipation of bioactive geometries produced by induced fit (see item 4.2) it will allow the user to infer a conformational selection process, given the identification of ligand-receptor complexes with the corresponding bioactive conformations.[75] In fact, conformational selection may be far more common than usually believed.[76,77] Additional applications of MD simulations of uncomplexed drug-like compounds include: (*i*) elucidation of NMR conformational information of peptides (mainly through

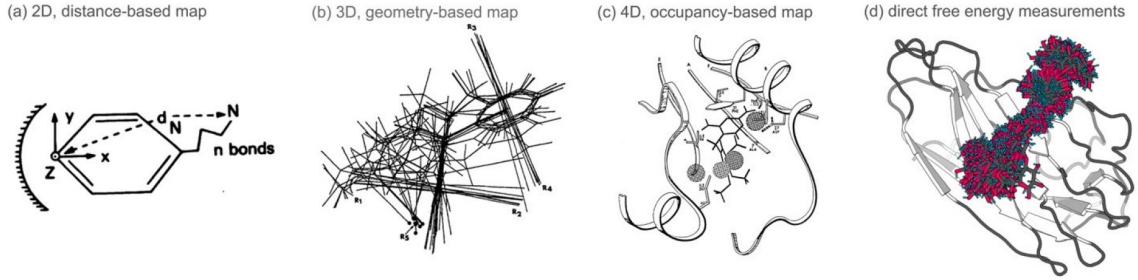

Figure 4. Evolution of models for ligand-receptor affinity inference. (a) A pharmacophoric model based on simple geometric descriptors, from the end of the 1970's (reproduced from reference 67 with copyright permission 2023 from Wiley Company). (b) 3D pharmacophoric model derived from the superimposition of multiple structures, from the late 1980's (reproduced from reference 68 with copyright permission 2023 from Wiley Company). (c) 4D formalism proposed by Hopfinger *et al*.[69] for the representation of ligand-receptor interactions, from the late 1990's (reproduced from reference 69 with copyright permission 2023 from American Chemical Society). (d) The current sampling of ligand-receptor complex by molecular simulations (MS), allowing the characterization of complex ensembles and main conformational states, for which accurate free energy estimations are becoming increasingly routine for medicinal chemists.

nuclear Overhauser effect (NOE) distances and $J^3_{H,H}$ couplings);[74,78,79] (*ii*) exploration of conformational differences between organic solvents used in NMR and water,[74] and (*iii*) identification of non-biological, crystal packing effects.[75,80-84]

4. Molecular Flexibility Impact on SBDD

4.1. Ligand dynamics

The addition of flexibility to ligand-receptor complexes (of experimental or computational origin) may promote significant conformational and orientational changes of the ligand,[85,86] which in turn will impact the definition and representation of pharmacophoric groups, the identification of binding pockets, and thereby the determination of a SAR. In this sense, the user must refrain from using only the last conformation of a simulation, since such an approach would eliminate the entire ensemble. There is no reason to distinguish the last conformation from the rest of the trajectory. Averaged data, as for interaction energies between amino acid residues and ligands, can be important tools to identify the main regions of both ligand and receptor that participate in complexation. However, averages may include substantial fluctuations of the properties being observed. For example, the side chain from an arginine residue at the binding site could fluctuate and interact with different parts of the ligand during the simulation. The identification of these interactions could be important in establishing SAR, but an average structure could represent a geometry that does not show any of these interactions or even having no physical meaning; for instance, a flipping aromatic ring has an average position of a single straight line. Alternatively, the identification of the main conformational states and interactions that are modeled during the simulation may be possible (for instance, through PCA or clustering). This, however, requires a careful selection of states to avoid fortuitous correlations with the experimental data. Recent approaches, such as the use of Markov state models,[87,88] may obviate the subjectivity of these analyses, but are still computationally costly and instrumentally challenging in the context of drug discovery pipelines.

4.2. Induced fit, allosterism, and intrinsic activity

The concept of allosterism was proposed in 1961,[89] based on the Greek words *allo* (meaning other, different) and *steric* (meaning "solid"), without direct structural evidence.[90] Two years later, Richard Feynman stated that "... everything that living things do can be understood in terms of the jigglings and wigglings of atoms".[91] But not until 1977 was it feasible to model such behavior through the first molecular dynamics simulation of a protein.[6] In the context of drug activity, the concept of allosterism intertwines with other phenomena such as the induced fit originally proposed in 1958,[7] the intrinsic activity of drugs (i.e., agonism/antagonism/inverse agonism), and ultimately with intrinsically disordered proteins,[92] in the sense that a series of conformational events, modifications in the protein flexibility[93] or in protein correlated motions[94] are triggered by drug complexation to its target protein.

Accurate representations of conformational events produced by drug action on target proteins have been described for multiple molecular systems by using different simulation approaches. Molecular systems that have drawn particular interest include conformational modulation of GPCRs[95-98] due to their importance to therapeutics; nAChR;[99,100] antithrombin activation by heparin;[101-103] modulation of kinases;[104-106] and CRISPR-Cas9 (clustered regularly interspaced short palindromic repeats and CRISPR-associated protein 9) function;[107] among many others. While these applications of MS require substantially longer time durations, and are therefore usually unsuitable for compound screening, they can significantly enable medicinal chemists to go beyond ligand binding and towards drug activity, particularly when backed by control simulations for negative (uncomplexed protein) and positive (known ligand) controls. Additionally, some of the previously mentioned enhanced sampling techniques may substantially reduce time scale limitations of conventional MD while accelerating drug discovery pipelines, whereas it remains to be determined if these algorithms will maintain a proper ensemble in which the enthalpic and entropic effects associated to allostery events could be observed.

4.3. Affinity prediction

The more common methods used by medicinal chemists to estimate the free energy of ligand binding can be grouped into two approaches: (*i*) end-state methods, such as the linear interaction energy approach (LIE)[108] and the molecular mechanics Poisson Boltzmann/generalized born surface area (MM-PB/GBSA);[109,110] and (*ii*) alchemical methods, such as thermodynamic integration (TI),[111] free energy perturbation (FEP)[112] and the Bennett[113] acceptance ratio method (BAR). Going beyond the methodology[114-117] and use[118] of these techniques, which have been reviewed regularly, our focus will be on the recent advances of their accuracies when predicting experimentally determined affinities. The role of ligand-receptor affinity as a key indicator of drug potency[46] supports the development of

more accurate drug-receptor modeling in drug discovery pipelines but, in this sense, the user must be also aware that experimentally determined affinities also have errors, whose magnitude will depend on the employed technique. Therefore, the discussion and pursue of more accurate simulation techniques will be likely limited to the experimental accuracy.

End-state methods correspond to simpler and comparatively computationally inexpensive techniques that are usually less accurate.[116] Additionally, several challenges may directly impact the quality of their results. For example, the predicted energies obtained through LIE can fluctuate substantially during simulations,[119] and longer simulations can in fact produce worse results, as the energy distribution becomes multimodal and linear responses are not able to represent the affinities anymore.[120] Higher accuracy has been associated to a specific and system-dependent calibration of LIE equation parameters.[121] To improve LIE accuracy and dependence on specific parameterization, variants such as its hybridization with GBSA (GBS-LIE) have been proposed, and have produced accuracies of up to 70% for three receptors and a couple of ligands while increasing speed by an order of magnitude compared to other LIE implementations.[122] The extended linear interaction energy (ELIE)[123] approach is an alternative that has achieved predictions similar to some alchemical methods, with accuracies ranging from 39 to 75%, depending on the molecular system. Other approaches focused on the reduction of the importance of the initial pose for predictions accuracies through multiple independent MD simulations to obtain weighted ensemble averages to be used in the LIE method, achieving errors smaller than 3 kJ mol^{-1}.[120]

Another end-point method to estimate ligand free energy, MM-PB/GBSA, has become popular in drug discovery projects.[124] This method is sometimes applied directly on docking-obtained poses (rescoring) and even on energy-minimized complexes, bringing the promise of fast and accurate predictions to drug discovery pipelines. Nonetheless, its accuracy in estimating absolute free energies has been commonly overestimated by users. While some authors consider MM-PB/GBSA as a potentially better tool than most scoring functions,[125] new docking scoring functions such as BT-Score, RF::VinaElemen, DockThor-RF, and RF::Khamis exhibit accuracies to predict affinities of up to 70% when tested against ca. 200 protein-ligand complexes retrieved from PDBbind 2013 Core Set (version 2013).[126,127] These alternatives demonstrate solid performance among a wide range of molecular systems, showing accuracies substantially higher than those of standard Vina and AutoDock[128] scoring functions, as well as some known functions from packages such as Sybyl, MOE and GOLD,[127] even though local Vina and Autodock have been largely employed as references to show the supposed advantages of rescoring docking poses by using MM-PB/GBSA, which could lead to a circumstantial perception of accuracy (added by smaller data sets of similar compounds).[125,129-131] Additionally, the accuracy of the poses selected from the docking (or even MD) methods as entries will strongly influence free-energy estimations.[132] Nevertheless, optimization of simulation parameters has been attempted to improve accuracy,[133] and higher accuracies have depended on the molecular system under study.[132,134]

The accuracies of both LIE (mainly through its variants) and MM-PB/GBSA have improved substantially in recent years, and can currently accommodate large sets of compounds compatible with the screening phase. However, the user should be aware that the accuracy of these methods is highly dependent on the specific molecular system and the chemical diversity of the ligands under study.[135] Consequently, the user must exercise caution when extrapolating previously described accuracies from different molecular systems. Also, the inverse relationship between docking speed and accuracy during the screening phase is far from consolidated; in order words, some scoring functions allow a very fast virtual screening, with a high level of confidence. It is important to realize that end-state methods assume that simulations of both complexed and uncomplexed states are representative of interactions under biological conditions,[116] which may not be the case (e.g., is it the ensemble able to identify the bioactive conformation?). Additional factors that may influence these end-state methods include the quality of the docking pose or crystal structure and the discontinuity of parameters between docking and MD force fields that may produce ligand reorientation at the binding site during simulations and consequently complicate the selection of a conformation for free energy estimation. A similar situation can be observed in molecular systems that are more prone to an induced fit recognition, in which major conformational changes may be identified upon complexation.[136] Therefore, longer simulations, which are potentially associated with larger conformational changes, have not been consistently more accurate in free energy predictions;[120,123] first, because they may not be sampling the bioactive, induced state and second, because the bioactive state may appear as noise in longer simulations as an underrepresented state.

In the case of alchemical transformation approaches, a more thorough theoretical background is applied, allowing the user to obtain relative free energy estimations for a series of similar compounds through a progressive

alchemical transformation between the ligands of the series. Being traditionally more computationally demanding and methodologically challenging, more recent automated procedures may facilitate the application of these techniques and the standardization of procedures, thus reducing the risk of human error and subsequently improving accuracy,[137-139] among other advantages.[116] Recent applications of free energy perturbation methods (FEP) yielded highly accurate predictions of the binding free energies of ca. 200 compounds with over 8 different target receptors, with errors within 1.0 kcal mol^{-1} of their experimental values.[115,140,141] On the other hand, results were highly dependent on the employed parameters, with OPLS2.1 solidly outperforming AM1-BCC/GAFF, ChelpG/CharmM,[142] MM/PBSA, and MM/GBSA.[143] Nonetheless, aspects such as the treatment of water molecules, the degree of sampling, and charge changes during alchemical transformations affect accuracy;[59,116] a promise tool to explore the role of water molecules on these processes is A-EDS,[59] a one-step perturbation method able to determine the presence of water molecules in the active site by probing them in a fast and straightforward way.[144]

4.4. Docking refinement

One of the main applications of MD simulations in drug discovery is the refinement of ligand-receptor complexes obtained by docking calculations. The simulation of a ligand dynamic at its binding site, starting from either X-ray crystallography or docking pose, can significantly change the predicted intermolecular interactions associated with molecular recognition, in which the ligand can change its position.[145] Amino acid residues from the receptor can dynamically interact with multiple groups of the ligand;[101] in some situations, the ligand may dissociate from the binding site.

On the other hand, while the use of MD simulations to refine docking poses can enrich our understanding of the molecular recognition under study, the observation of ligand dissociation may arise from multiple factors, such as poorly executed docking, erroneous amino acid ionization (particularly for histidines), or poor equilibration prior to the simulation (extremely common, as discussed above). Furthermore, a precise determination of a ligand time of residence would require an extremely robust sampling of the system, including much longer or multiple simulations (starting from different velocities) to eliminate random and rare events, or even enhanced sampling techniques such as steered molecular dynamics (SMD),[146,147] among other approaches.[148] Therefore, the concept that MD simulation will validate docking results can be misleading, to say the least.

In fact, the time required for a ligand to dissociate from its target receptor is generally not a good predictor of ligand affinity.[149] From an historical perspective, as early as 1986, Leysen and Gommeren[149] tested the binding of a series of compounds against serotonin S_2, dopamine D_2, histamine H_1, adrenergics α_1 and α_2, and opiate μ receptors while considering both affinities and dissociation times. Affinities ranged from 0.4 to 8,000 nM, while dissociation times varied from 1.9 to 260 min. No correlation was observed between the two properties, indicating that the time a compound requires to dissociate from its target receptor is not directly related to its affinity. More importantly, in spite of being mostly neglected on drug discovery pipelines, a drug-receptor residence time may be a better predictor of *in vivo* efficacy when compared to classical drug affinity parameters,[150] and recent works[151] have been advancing on the development of accurate simulation protocols to describe it. Also, the dissociation time should be within the simulation time, which is usually not the case.[149] The situation was similar for other GPCRs, including M_3, D_2, NK_1, and CRF_1 receptors.[152] Considering $K_d = K_{off}/K_{on}$ (K_d being the equilibrium dissociation constant, K_{off} dissociation rate constant and K_{on} the association rate constant), and an average value for K_{on} of 10^8 M^{-1} s^{-1} (taking as reference β_2-adrenoreceptor modulators),[153] the dissociation of a ligand within simulations of 100 ns would imply in extremely low affinity ligands ($K_d = 0.1$ M), which is not realistic considering drug-like prototypes. As a consequence, if there is evidence for appreciable affinity for a given ligand-receptor system, the dissociation of a ligand during most MD timescales is more likely to be due to problems in the simulation setup (such as the docking pose, protonation states, equilibration and force field among others) then due to an (artificially) low affinity.

5. Future Prospects

Recent advances have brought MS into key roles in drug discovery and development in academic, industrial, and clinical communities. Consequently, improved accuracy, precision, reproducibility, and timescales compatible with decision making will be expected.[46] In this context, a recent editorial from the *Journal of Chemical Information and Modeling* by Soares *et al.*[45] regarding guidelines for reporting molecular dynamics simulations data emphasized important directions for future studies, such as the use of replica simulations to increase sampling,[46] combined with enhanced sampling techniques to facilitate the crossing of high energy barriers, and validated to the greatest possible

extent by experimental data. Although significant advances have increased both the accuracy and effectiveness of alchemical free-energy techniques for the prediction of ligand binding, and because these methods are assuming a vital role in the pharmaceutical industry,[154] an important consideration is that the magnitude of error of most approaches may still impose semi-quantitative analyses of predictions, as of the prediction of nonbinders.[108]

The upcoming decades will likely see a growing set of developments that may improve sampling, accuracy, operability, and the interpretation of simulation data, such as:

(*i*) Increase in software and hardware acceleration, including a growing role of GPU;

(*ii*) continuous growth of simulation lengths, allowing users to achieve time scales of some biological phenomena by using conventional MD;

(*iii*) common use of replicas and reference simulations. Control simulations (positive and negative) will assume a growing importance to data analysis and model accuracy;

(*iv*) progressive popularization of enhanced sampling techniques, reducing the limitation of simulation lengths from conventional MD;

(*v*) machine-learning and artificial intelligence models will play a growing role on MS, both substituting current energy functions by ML-derived potentials with QM accuracy and allowing improved free energy predictions, while reducing the dependence of simulation setup and data interpretation on user experience and know-how.

(*vi*) and, most importantly, a continuous improvement of model accuracy, allowing users to focus on progressively more complex questions at increasingly speeds to fight disease and enhance population health.

Acknowledgments

The authors thank the Brazilian research funding agencies Coordenação de Aperfeiçoamento de Pessoal de Nível Superior (CAPES), Conselho Nacional de Desenvolvimento Científico e Tecnológico (CNPq), Fundação de Amparo à Pesquisa do Estado do Rio Grande do Sul (FAPERGS), Instituto Nacional de Ciência e Tecnologia em Biologia do Câncer Infantil e Oncologia Pediátrica - INCT BioOncoPed, process CNPq No. 406484/2022-8, the Laboratório Nacional de Computação Científica (LNCC/MCTI, Brazil) for the use of the Santos Dumont supercomputer and the financial support by the Austrian Federal Ministry for Digital and Economic Affairs, the National Foundation for Research, Technology and Development and the Christian Doppler Research Association is gratefully acknowledged. The authors also thanks Lais Barth Arent, João Carlos Rodrigues Junior, and Vinicius Cabral Avila for their assistance in collecting bibliometric data.

Author Contributions

Hugo Verli was responsible for conceptualization, data curation, formal analysis, funding acquisition, investigation, project administration, resources, software, visualization, writing (original draft, review and editing); Chris Oostenbrink for conceptualization, resources, funding acquisition, writing (original draft, review and editing).

Hugo Verli *obtained his MSc in UFRJ (2001) and his PhD in UFRGS (2005). Since 2006 he holds a position at UFRGS for Bioinformatics, being a Full Professor since 2022. He was an affiliated member of the Brazilian Academy of Sciences (2012-2016), Coordinator of the Graduate Program in Cell and Molecular Biology (UFRGS, 2020-2023), and is currently the vice director of Center for Biotechnology (UFRGS) and member of the INCT BioOncoPed. Supervised around 40 PhD and MSc students, publishing over 100 peer-reviewed papers on molecular simulations, on the field of computational simulations of biomolecular dynamics in solution.*

Chris Oostenbrink *studied at VU University in Amsterdam (MSc 2000) and did his PhD 2004 at the ETH in Zurich. From 2004 to 2009 he was assistant professor at VU University, leading the computational chemistry unit at the division of molecular and computational toxicology. In 2009, he moved to BOKU University in Vienna, where he holds a chair for biomolecular modeling and simulation. He was a recipient of a Starting Grant of the European Research Council (ERC). He has published over 200 peer-reviewed papers involving computational approaches to describe complex biomolecular systems, free-energy techniques and enhanced sampling.*

References

1. Barton, D. H. R.; Cookson, R. C.; *Q. Rev., Chem. Soc.***1956**, *10*, 44. [Crossref]
2. Haworth, W. N.; *The Constitution of Sugars*; Edwnrd Arnold & Co.: London, 1929 (*CA 23:16254*).
3. Anfinsen, C. B.; Haber, E.; Sela, M.; White, F. H.; *Proc. Natl. Acad. Sci. U. S. A.* **1961**, *47*, 1309. [Crossref]

4. Levinthal, C.; *Sci. Am.* **1966**, *214*, 42. [Crossref]
5. Levitt, M.; Warshel, A.; *Nature* **1975**, *253*, 694. [Crossref]
6. McCammon, J. A.; Gelin, B. R.; Karplus, M.; *Nature* **1977**, *267*, 585. [Crossref]
7. Koshland Jr., D. E.; *Proc. Natl. Acad. Sci. U. S. A.* **1958**, *44*, 98. [Crossref]
8. Burgen, A. S. V.; Roberts, G. C. K.; Feeney, J.; *Nature* **1975**, *253*, 753. [Crossref]
9. Copeland, R. A.; Pompliano, D. L.; Meek, T. D.; *Nat. Rev. Drug Discovery* **2006**, *5*, 730. [Crossref]
10. Jorgensen, W. L.; *Science* **2004**, *303*, 1813. [Crossref]
11. Hardy, L. W.; Malikayil, A.; *Curr. Drug Discovery* **2003**, 15. [Link] accessed in June 2024.
12. Saikia, S.; Bordoloi, M.; *Curr. Drug Targets* **2019**, *20*, 501. [Crossref]
13. Tian, C.; Kasavajhala, K.; Belfon, K. A. A.; Raguette, L.; Huang, H.; Migues, A. N.; Bickel, J.; Wang, Y.; Pincay, J.; Wu, Q.; Simmerling, C.; *J. Chem. Theory Comput.* **2020**, *16*, 528. [Crossref]
14. Huang, J.; Rauscher, S.; Nawrocki, G.; Ran, T.; Feig, M.; De Groot, B. L.; Grubmüller, H.; MacKerell Jr., A. D.; *Nat. Methods* **2017**, *14*, 71. [Crossref]
15. Reif, M. M.; Hunenberger, P. H.; Oostenbrink, C.; *J. Chem. Theory Comput.* **2012**, *8*, 3705. [Crossref]
16. Harder, E.; Damm, W.; Maple, J.; Wu, C.; Reboul, M.; Xiang, J. Y.; Wang, L.; Lupyan, D.; Dahlgren, M. K.; Knight, J. L.; Kaus, J. W.; Cerutti, D. S.; Krilov, G.; Jorgensen, W. L.; Abel, R.; Friesner, R. A.; *J. Chem. Theory Comput.* **2016**, *12*, 281. [Crossref]
17. Hendrickson, J. B.; *J. Am. Chem. Soc.* **1961**, *83*, 4537. [Crossref]
18. Wertz, D. H.; Allinger, N. L.; *Tetrahedron* **1974**, *30*, 1579. [Crossref]
19. Allinger, N. L.; Yan, L.; *J. Am. Chem. Soc.* **1993**, *115*, 11918. [Crossref]
20. Halgren, T. A.; *J. Comput. Chem.* **1996**, *17*, 490. [Crossref]
21. Santos, K. B.; Guedes, I. A.; Karl, A. L. M.; Dardenne, L. E.; *J. Chem. Inf. Mod.* **2020**, *60*, 667. [Crossref]
22. Wang, J.; Wolf, R. M.; Caldwell, J. W.; Kollman, P. A.; Case, D. A.; *J. Comp. Chem.* **2004**, *25*, 1157. [Crossref]
23. Vanommeslaeghe, K.; MacKerell, A. D.; *J. Chem. Inf. Mod.* **2012**, *52*, 3144. [Crossref]
24. Vanommeslaeghe, K.; Raman, E. P.; MacKerell, A. D.; *J. Chem. Inf. Mod.* **2012**, *52*, 3155. [Crossref]
25. Lee, J.; Cheng, X.; Swails, J. M.; Yeom, M. S.; Eastman, P. K.; Lemkul, J. A.; Wei, S.; Buckner, J.; Jeong, J. C.; Qi, Y.; Jo, S.; Pande, V. S.; Case, D. A.; Brooks, C. L.; MacKerell, A. D.; Klauda, J. B.; Im, W.; *J. Chem. Theory Comp.* **2016**, *12*, 405. [Crossref]
26. Schuttelkopf, A. W.; van Aalten, D. M. F.; *Acta Crystallogr., Sect. D: Biol. Crystallogr.* **2004**, *60*, 1355. [Crossref]
27. Stroet, M.; Caron, B.; Visscher, K. M.; Geerke, D. P.; Malde, A. K.; Mark, A. E.; *J. Chem. Theory Comp.* **2018**, *14*, 5834. [Crossref]
28. Amber, ambermd.org, accessed in June 2024.
29. CHARMM, academiccharmm.org, accessed in June 2024.
30. Schrodinger, www.schrodinger.com, accessed in June 2024.
31. GROMACS, www.gromacs.org, accessed in June 2024.
32. GROMOS, www.gromos.net, accessed in June 2024.
33. NAMD - Scalable Molecular Dynamics, www.ks.uiuc.edu/Research/namd, accessed in June 2024.
34. OpenMM, openmm.org, accessed in June 2024.
35. Rackers, J. A.; Wang, Z.; Lu, C.; Laury, M. L.; Lagardère, L.; Schnieders, M. J.; Piquemal, J. P.; Ren, P.; Ponder, J. W.; *J. Chem. Theor. Comp.* **2018**, *14*, 5273. [Crossref]
36. Talirz, L.; Ghiringhelli, L. M.; Smit, B.; *Living J. Comp. Mol. Sci.* **2021**, *3*, 1483. [Crossref]; Trends in Atomistic Simulation Engines, https://atomistic.software/#/, accessed in June 2024.
37. Stewart, J. J. P.; *J. Mol. Struct.* **1997**, *401*, 195. [Crossref]
38. Ligabue-Braun, R.; Sachett, L. G.; Pol-Fachin, L.; Verli, H.; *Plos One* **2015**, *10*, e0132311. [Crossref]
39. Devereux, C.; Smith, J. S.; Huddleston, K. K.; Barros, K.; Zubatyuk, R.; Isayev, O.; Roitberg, A. E.; *J. Chem. Theory Comp.* **2020**, *16*, 4192. [Crossref]
40. van Gunsteren, W. F.; Daura, X.; Hansen, N.; Mark, A. E.; Oostenbrink, C.; Riniker, S.; Smith, L. J.; *Angew. Chem., Int. Ed.* **2018**, *57*, 884. [Crossref]
41. Salsbury Jr., F. R.; *Curr. Opin. Pharmacol.* **2010**, *10*, 738. [Crossref]
42. Kunz, A. P. E.; Van Gunsteren, W. F.; *J. Phys. Chem. A* **2009**, *113*, 11570. [Crossref]
43. Cabral, A. V.; Govoni, B.; Verli, H.; *Carbohydr. Pol.* **2024**, 121792. [Crossref]
44. Tummino, P. J.; Copeland, R. A.; *Biochemistry* **2008**, *47*, 5481. [Crossref]
45. Soares, T. A.; Cournia, Z.; Naidoo, K.; Amaro, R.; Wahab, H.; Merz Jr., K. M.; *J. Chem. Inf. Model.* **2023**, *63*, 3227. [Crossref]
46. Wan, S.; Bhati, A. P.; Zasada, S. J.; Coveney, P. V.; *Interface Focus* **2020**, *10*, 20200007. [Crossref]
47. Huber, T.; Torda, A. E.; van Gunsteren, W. F.; *J. Computer-Aided Mol. Des.* **1994**, *8*, 695. [Crossref]
48. Laio, A.; Parrinello, M.; *Proc. Natl. Acad. Sci. U. S. A.* **2002**, *99*, 12562. [Crossref]
49. Ray, D.; Parrinello, M.; *J. Chem. Theory Comput.* **2023**, *19*, 5649. [Crossref]
50. Hukushima, K.; Nemoto, K.; *J. Phys. Soc. Jpn.* **1996**, *65*, 1604. [Crossref]
51. Bernardi, R. C.; Melo, M. C. R.; Schulten, K.; *Biochim. Biophys. Acta, Gen. Subj.* **2015**, *1850*, 872. [Crossref]
52. Miao, Y.; Feher, V. A.; McCammon, J. A.; *J. Chem. Theory Comput.* **2015**, *11*, 3584. [Crossref]
53. Wang, J.; Arantes, P. R.; Bhattarai, A.; Hsu, R. V.; Pawnikar, S.; Huang, Y. M.; Palermo, G.; Miao, Y.; *WIREs Comput. Mol. Sci* **2021**, *11*, e1521. [Crossref]

54. Bahar, I.; Lezon, T. R.; Bakan, A.; Shrivastava, I. H.; *Chem. Rev.* **2010**, *110*, 1463. [Crossref]
55. Moroy, G.; Sperandio, O.; Rielland, S.; Khemka, S.; Druart, K.; Goyal, D.; Perahia, D.; Miteva, M. A.; *Future Med. Chem.* **2015**, *7*, 2317. [Crossref]
56. Costa, M. G. S.; Batista, P. R.; Bisch, P. M.; Perahia, D.; *J. Chem. Theory Comp.* **2015**, *11*, 2755. [Crossref]
57. Torrie, G. M.; Valleau, J. P.; *J. Comp. Phys.* **1977**, *23*, 187. [Crossref]
58. Kästner, J.; *WIREs Comput. Mol. Sci.* **2011**, *1*, 932. [Crossref]
59. Gracia Carmona, O.; Oostenbrink, C.; *J. Chem. Inf. Model.* **2023**, *63*, 197. [Crossref]
60. Tribello, G. A.; Bonomi, M.; Branduardi, D.; Camilloni, C.; Bussi, G.; *Comput. Phys. Commun.* **2014**, *185*, 604. [Crossref]
61. ithub.com/mcosta27/MDexciteR, accessed in June 2024.
62. Christen, M.; van Gunsteren, W. F.; *J. Comput. Chem.* **2008**, *29*, 157. [Crossref]
63. Jumper, J.; Evans, R.; Pritzel, A.; Green, T.; Figurnov, M.; Ronneberger, O.; Tunyasuvunakool, K.; Bates, R.; Žídek, A.; Potapenko, A.; Bridgland, A.; Meyer, C.; Kohl, S. A. A.; Ballard, A. J.; Cowie, A.; Romera-Paredes, B.; Nikolov, S.; Jain, R.; Adler, J.; Back, T.; Petersen, S.; Reiman, D.; Clancy, E.; Zielinski, M.; Steinegger, M.; Pacholska, M.; Berghammer, T.; Bodenstein, S.; Silver, D.; Vinyals, O.; Senior, A. W.; Kavukcuoglu, K.; Kohli, P.; Hassabis, D.; *Nature* **2021**, *596*, 583. [Crossref]
64. Lensink, M. F.; Brysbaert, G.; Raouraoua, N.; Bates, P. A.; Giulini, M.; Honorato, R. V.; van Noort, C.; Teixeira, J. M. C.; Bonvin, A. M. J. J.; Kong, R.; Shi, H.; Lu, X.; Chang, S.; Liu, J.; Guo, Z.; Chen, X.; Morehead, A.; Roy, R. S.; Wu, T.; Giri, N.; Quadir, F.; Chen, C.; Cheng, J.; Del Carpio, C. A.; Ichiishi, E.; Rodriguez-Lumbreras, L. A.; Fernandez-Recio, J.; Harmalkar, A.; Chu, L.-S.; Canner, S.; Smanta, R.; Gray, J. J.; Li, H.; Lin, P.; He, J.; Tao, H.; Huang, S.-Y.; Roel-Touris, J.; Jimenez-Garcia, B.; Christoffer, C. W.; Jain, A. J.; Kagaya, Y.; Kannan, H.; Nakamura, T.; Terashi, G.; Verburgt, J. C.; Zhang, Y.; Zhang, Z.; Fujuta, H.; Sekijima, M.; Kihara, D.; Khan, O.; Kotelnikov, S.; Ghani, U.; Padhorny, D.; Beglov, D.; Vajda, S.; Kozakov, D.; Negi, S. S.; Ricciardelli, T.; Barradas-Bautista, D.; Cao, Z.; Chawla, M.; Cavallo, L.; Oliva, R.; Yin, R.; Cheung, M.; Guest, J. D.; Lee, J.; Pierce, B. G.; Shor, B.; Cohen, T.; Halfon, M.; Schneidman-Duhovny, D.; Zhu, S.; Yin, R.; Sun, Y.; Shen, Y.; Maszota-Zieleniak, M.; Bojarski, K. K.; Lubecka, E. A.; Marcisz, M.; Danielsson, A.; Dziadek, L.; Gaardlos, M.; Gieldon, A.; Liwo, A.; Samsonov, S. A.; Slusarz, R.; Zieba, K.; Sieradzan, A. K.; Czaplewski, C.; Kobayashi, S.; Miyakawa, Y.; Kiyota, Y.; Takeda-Shitaka, M.; Olechnovic, K.; Valancauskas, L.; Dapkunas, J.; Venclovas, C.; Wallner, B.; Yang, L.; Hou, C.; He, X.; Guo, S.; Jiang, S.; Ma, X.; Duan, R.; Qui, L.; Xu, X.; Zou, X.; Velankar, S.; Wodak, S. J. ; *Proteins: Struct., Funct., Bioinf.* **2023**, *91*, 1658. [Crossref]
65. Ovchinnikov, S.; Kinch, L.; Park, H.; Liao, Y.; Pei, J.; Kim, D. E.; Kamisetty, H.; Grishin, N. V.; Baker, D.; *eLife* **2015**, *4*, e09248. [Crossref]
66. Waterhouse, A.; Bertoni, M.; Bienert, S.; Studer, G.; Tauriello, G.; Gumienny, R.; Heer, F. T.; de Beer, T. A. P.; Rempfer, C.; Bordoli, L.; Lepore, R.; Schwede, T.; *Nucleic Acids Res.* **2018**, *46*, W296. [Crossref]
67. Schwalbe, C. H.; Scott, D. K.; *Br. J. Pharmacol.* **1979**, *66*, 403P (*CA 92:52189*).
68. Andrews, P. R.; Craik, D. J.; Munro, S. L.; *Quant. Struct.-Act. Relat.* **1987**, *6*, 97. [Crossref]
69. Hopfinger, A. J.; Wang, S.; Tokarski, J. S.; Jin, B.; Albuquerque, M.; Madhav, P. J.; Duraiswami, C.; *J. Am. Chem. Soc.* **1997**, *119*, 10509. [Crossref]
70. Hawkins, P. C. D.; *J. Chem. Inf. Model.* **2017**, *57*, 1747. [Crossref]
71. McNutt, A. T.; Bisiriyu, F.; Song, S.; Vyas, A.; Hutchison, G. R.; Koes, D. R.; *J. Chem. Inf. Model.* **2023**, *63*, 6598. [Crossref]
72. Bak, A.; *Int. J. Mol. Sci.* **2021**, *22*, 5212. [Crossref]
73. Sheridan, R. P.; Nilakantan, R.; Dixon, J. S.; Venkataraghavan, R.; *J. Med. Chem.* **1986**, *29*, 899. [Crossref]
74. Arantes, P. R.; Polêto, M. D.; John, E. B. O.; Pedebos, C.; Grisci, B. I.; Dorn, M.; Verli, H.; *J. Phys. Chem. B* **2019**, *123*, 994. [Crossref]
75. Tesch, R.; Becker, C.; Müller, M. P.; Beck, M. E.; Quambusch, L.; Getlik, M.; Lategahn, J.; Uhlenbrock, N.; Costa, F. N.; Polêto, M. D.; Pinheiro, P. de S. M.; Rodrigues, D. A.; Sant'Anna, C. M. R.; Ferreira, F. F.; Verli, H.; Fraga, C. A. M.; Rauh, D.; *Angew. Chem., Int. Ed.* **2018**, *57*, 9970. [Crossref]
76 Vogt, A. D.; Di Cera, E.; *Biochemistry* **2012**, *51*, 5894. [Crossref]
77. Hritz, J.; Läppchen, T.; Oostenbrink, C.; *Eur. Biophys. J.* **2010**, *39*, 1573. [Crossref]
78. Cardoso, C. L.; Castro-Gamboa, I.; Bergamini, G. M.; Cavalheiro, A. J.; Silva, D. H. S.; Lopes, M. N.; Araújo, A. R.; Furlan, M.; Verli, H.; Bolzani, V. S.; *J. Nat. Prod.* **2011**, *74*, 487. [Crossref]
79. Altei, W. F. F.; Picchi, D. G. G.; Abissi, B. M. M.; Giesel, G. M. M.; Flausino Jr., O.; Reboud-Ravaux, M.; Verli, H.; Crusca, E.; Silveira, E. R. R.; Cilli, E. M. M.; Bolzani, V. S. S.; Flausino, O.; Reboud-Ravaux, M.; Verli, H.; Crusca, E.; Silveira, E. R. R.; Cilli, E. M. M.; Bolzani, V. S. S.; *Phytochemistry* **2014**, *107*, 91. [Crossref]
80. Adachi, N.; Yamaguchi, T.; Moriya, T.; Kawasaki, M.; Koiwai, K.; Shinoda, A.; Yamada, Y.; Yumoto, F.; Kohzuma, T.; Senda, T.; *J. Struct. Biol.* **2021**, *213*, 107768. [Crossref]
81. Coskun, D.; Chen, W.; Clark, A. J.; Lu, C.; Harder, E. D.; Wang, L.; Friesner, R. A.; Miller, E. B.; *J. Chem. Theory Comput.* **2022**, *18*, 7193. [Crossref]
82. Wang, P.; Dhananjayan, N.; Hagras, M. A.; Stuchebrukhov, A. A.; *Biochim. Biophys. Acta, Bioenerg.* **2021**, *1862*, 148326. [Crossref]

83. Camargo, S.; Mulinari, E. J.; de Almeida, L. R.; Bernardes, A.; Prade, R. A.; Garcia, W.; Segato, F.; Muniz, J. R. C.; *Biochim. Biophys. Acta, Proteins Proteomics* **2020**, *1868*, 140533. [Crossref]
84. Rai, B. K.; Sresht, V.; Yang, Q.; Unwalla, R.; Tu, M.; Mathiowetz, A. M.; Bakken, G. A.; *J. Chem. Inf. Model.* **2019**, *59*, 4195. [Crossref]
85. Lima, L. M. T.; Becker, C. F. F.; Giesel, G. M. M.; Marques, A. F. F.; Cargnelutti, M. T. T.; Neto, M. O.; Monteiro, R. Q.; Verli, H.; Polikarpov, I.; *Biochim. Biophys. Acta, Proteins Proteomics* **2009**, *1794*, 873. [Crossref]
86. Giesel, G.; Lima, L.; Faberbarata, J.; Guimaraes, J. A.; Verli, H.; *FEBS Lett.* **2008**, *582*, 3619. [Crossref]
87. Husic, B. E.; Pande, V. S.; *J. Am. Chem. Soc.* **2018**, *140*, 2386. [Crossref]
88. Scherer, M. K.; Trendelkamp-Schroer, B.; Paul, F.; Pérez-Hernández, G.; Hoffmann, M.; Plattner, N.; Wehmeyer, C.; Prinz, J.-H.; Noé, F.; *J. Chem. Theory Comp.* **2015**, *11*, 5525. [Crossref]
89. Monod, J.; Jacob, F.; *Cold Spring Harbor Symp. Quant. Biol.* **1961**, *26*, 389. [Crossref]
90. Cui, Q.; Karplus, M.; *Prot. Sci.* **2008**, *17*, 1295. [Crossref]
91. Feynman, R. P.; Leighton, R. B.; Sands, M.; *The Feynman Lectures in Physics*, vol. 1; Addison-Wesley: Reading, UK, 1963, ch. 3.
92. Berlow, R. B.; Jane Dyson, H.; Wright, P. E.; *J. Mol. Biol.* **2018**, *430*, 2309. [Crossref]
93. Venäläinen, T.; Molnár, F.; Oostenbrink, C.; Carlberg, C.; Peräkylä, M.; *Proteins: Struct., Funct., Bioinf.* **2010**, *78*, 873. [Crossref]
94. Macpherson, J. A.; Theisen, A.; Masino, L.; Fets, L.; Driscoll, P. C.; Encheva, V.; Snijders, A. P.; Martin, S. R.; Kleinjung, J.; Barran, P. E.; Fraternali, F.; Anastasiou, D.; *eLife* **2019**, *8*, e45068. [Crossref]
95. Dror, R. O.; Arlow, D. H.; Maragakis, P.; Mildorf, T. J.; Pan, A. C.; Xu, H. F.; Borhani, D. W.; Shaw, D. E.; *Proc. Natl. Acad. Sci. U.S.A.* **2011**, *108*, 18684. [Crossref]
96. Massink, A.; Gutiérrez-de-Terán, H.; Lenselink, E. B.; Zacarías, N. V. O.; Xia, L.; Heitman, L. H.; Katritch, V.; Stevens, R. C.; IJzerman, A. P.; *Mol. Pharmacol.* **2015**, *87*, 305. [Crossref]
97. Rosenbaum, D. M.; Zhang, C.; Lyons, J. A.; Holl, R.; Aragao, D.; Arlow, D. H.; Rasmussen, S. G. F.; Choi, H.-J.; DeVree, B. T.; Sunahara, R. K.; Chae, P. S.; Gellman, S. H.; Dror, R. O.; Shaw, D. E.; Weis, W. I.; Caffrey, M.; Gmeiner, P.; Kobilka, B. K.; *Nature* **2011**, *469*, 236. [Crossref]
98. Huang, W.; Manglik, A.; Venkatakrishnan, A. J.; Laeremans, T.; Feinberg, E. N.; Sanborn, A. L.; Kato, H. E.; Livingston, K. E.; Thorsen, T. S.; Kling, R. C.; Granier, S.; Gmeiner, P.; Husbands, S. M.; Traynor, J. R.; Weis, W. I.; Steyaert, J.; Dror, R. O.; Kobilka, B. K.; *Nature* **2015**, *524*, 315. [Crossref]
99. Cheng, X. L.; Lu, B. Z.; Grant, B.; Law, R. J.; McCammon, J. A.; *J. Mol. Biol.* **2006**, *355*, 310. [Crossref]
100. Cheng, X.; Wang, H.; Grant, B.; Sine, S. M.; McCammon, J. A.; *PLoS Comput. Biol.* **2006**, *2*, 1173. [Crossref]
101. Verli, H.; Guimarães, J. A.; *J. Mol. Graphics Modell.* **2005**, *24*, 203. [Crossref]
102. Pol-Fachin, L.; Becker, C. F.; Guimarães, J. A.; Verli, H.; *Proteins: Struct., Funct., Bioinf.* **2011**, *79*, 2735. [Crossref]
103. Arantes, P. R.; Pérez-Sánchez, H.; Verli, H.; *J. Biomol. Struct. Dyn.* **2018**, *36*, 4045. [Crossref]
104. Ozkirimli, E.; Post, C. B.; *Protein Sci.* **2006**, *15*, 1051. [Crossref]
105. Nam, K.; Tao, Y.; Ovchinnikov, V.; *J. Phys. Chem. B* **2023**, *127*, 5789. [Crossref]
106. Olivieri, F. A.; Burastero, O.; Drusin, S.; Defelipe, L. A.; Wetzler, D. E.; Turjanski, A.; Marti, M.; *J. Chem. Inf. Model.* **2020**, *60*, 833. [Crossref]
107. Nierzwicki, L.; Arantes, P. R.; Saha, A.; Palermo, G.; *Wiley Interdiscip. Rev.: Comput. Mol. Sci.* **2021**, *11*, e1503. [Crossref]
108. Aqvist, J.; Medina, C.; Samuelsson, J. E.; *Protein Eng., Des. Sel.* **1994**, *7*, 385. [Crossref]
109. Srinivasan, J.; Cheatham, T. E.; Cieplak, P.; Kollman, P. A.; Case, D. A.; *J. Am. Chem. Soc.* **1998**, *120*, 9401. [Crossref]
110. Kollman, P. A.; Massova, I.; Reyes, C.; Kuhn, B.; Huo, S.; Chong, L.; Lee, M.; Lee, T.; Duan, Y.; Wang, W.; Donini, O.; Cieplak, P.; Srinivasan, J.; Case, D. A.; Cheatham, T. E.; *Acc. Chem. Res.* **2000**, *33*, 889. [Crossref]
111. Kirkwood, J. G.; *J. Chem. Phys.* **1935**, *3*, 300. [Crossref]
112. Zwanzig, R. W.; *J. Chem. Phys.* **1954**, *22*, 1420. [Crossref]
113. Bennett, C. H.; *J. Comp. Phys.* **1976**, *22*, 245. [Crossref]
114. Klimovich, P. V.; Shirts, M. R.; Mobley, D. L.; *J. Comput. Aided Mol. Des.* **2015**, *29*, 397. [Crossref]
115. Wang, L.; Wu, Y.; Deng, Y.; Kim, B.; Pierce, L.; Krilov, G.; Lupyan, D.; Robinson, S.; Dahlgren, M. K.; Greenwood, J.; Romero, D. L.; Masse, C.; Knight, J. L.; Steinbrecher, T.; Beuming, T.; Damm, W.; Harder, E.; Sherman, W.; Brewer, M.; Wester, R.; Murcko, M.; Frye, L.; Farid, R.; Lin, T.; Mobley, D. L.; Jorgensen, W. L.; Berne, B. J.; Friesner, R. A.; Abel, R.; *J. Am. Chem. Soc.* **2015**, *137*, 2695. [Crossref]
116. de Ruiter, A.; Oostenbrink, C.; *Curr. Opin. Struct. Biol.* **2020**, *61*, 207. [Crossref]
117. Cournia, Z.; Allen, B.; Sherman, W.; *J. Chem. Inf. Model.* **2017**, *57*, 2911. [Crossref]
118. Mey, A. S. J. S.; Allen, B. K.; Bruce Macdonald, H. E.; Chodera, J. D.; Hahn, D. F.; Kuhn, M.; Michel, J.; Mobley, D. L.; Naden, L. N.; Prasad, S.; Rizzi, A.; Scheen, J.; Shirts, M. R.; Tresadern, G.; Xu, H.; *Living J. Comput. Mol. Sci.* **2020**, *2*, 18378. [Crossref]
119. Sokouti, B.; Dastmalchi, S.; Hamzeh-Mivehroud, M.; *J. Bioinform. Comput. Biol.* **2022**, *20*, 2250024. [Crossref]
120. Stjernschantz, E.; Oostenbrink, C.; *Biophys. J.* **2010**, *98*, 2682. [Crossref]

121. Valdés-Tresanco, M. S.; Valdés-Tresanco, M. E.; Rubio-Carrasquilla, M.; Valiente, P. A.; Moreno, E.; *ACS Omega* **2021**, *6*, 29525. [Crossref]
122. Zhou, R.; Friesner, R. A.; Ghosh, A.; Rizzo, R. C.; Jorgensen, W. L.; Levy, R. M.; *J. Phys. Chem. B* **2001**, *105*, 10388. [Crossref]
123. He, X.; Man, V. H.; Ji, B.; Xie, X.-Q.; Wang, J.; *J. Comput. Aided Mol. Des.* **2019**, *33*, 105. [Crossref]
124. King, E.; Aitchison, E.; Li, H.; Luo, R.; *Front. Mol. Biosci.* **2021**, *8*, 712085. [Crossref]
125. Hu, X.; Contini, A.; *J. Chem. Inf. Mod.* **2019**, *59*, 2714. [Crossref]
126. PDBbind, http://www.pdbbind-cn.org/, accessed in June 2024.
127. Guedes, I. A.; Barreto, A. M. S.; Marinho, D.; Krempser, E.; Kuenemann, M. A.; Sperandio, O.; Dardenne, L. E.; Miteva, M. A.; *Sci. Rep.* **2021**, *11*, 3198. [Crossref]
128. Trott, O. E.; Olson, A.; *J. Comput. Chem.* **2010**, *31*, 455. [Crossref]
129. Hou, T.; Wang, J.; Li, Y.; Wang, W.; *J. Comp. Chem.* **2011**, *32*, 866. [Crossref]
130. Sgobba, M.; Caporuscio, F.; Anighoro, A.; Portioli, C.; Rastelli, G.; *Eur. J. Med. Chem.* **2012**, *58*, 431. [Crossref]
131. Zhang, X.; Wong, S. E.; Lightstone, F. C.; *J. Chem. Inf. Model.* **2014**, *54*, 324. [Crossref]
132. Yau, M. Q.; Emtage, A. L.; Chan, N. J. Y.; Doughty, S. W.; Loo, J. S. E.; *J. Comput. Aided Mol. Des.* **2019**, *33*, 487. [Crossref]
133. Valdés-Tresanco, M. E.; Valdés-Tresanco, M. S.; Moreno, E.; Valiente, P. A.; *J. Phys. Chem. B* **2023**, *127*, 944. [Crossref]
134. Yau, M. Q.; Emtage, A. L.; Loo, J. S. E.; *J. Comput. Aided Mol. Des.* **2020**, *34*, 1133. [Crossref]
135. Hou, T. J.; Wang, J. M.; Li, Y. Y.; Wang, W.; *J. Chem. Inf. Mod.* **2011**, *51*, 69. [Crossref]
136. Wan, S.; Bhati, A. P.; Skerratt, S.; Omoto, K.; Shanmugasundaram, V.; Bagal, S. K.; Coveney, P. V.; *J. Chem. Inf. Model.* **2017**, *57*, 897. [Crossref]
137. Jo, S.; Jiang, W.; Lee, H. S.; Roux, B.; Im, W.; *J. Chem. Inf. Model.* **2013**, *53*, 267. [Crossref]
138. Loeffler, H. H.; Michel, J.; Woods, C.; *J. Chem. Inf. Model.* **2015**, *55*, 2485. [Crossref]
139. Stroet, M.; Caron, B.; Visscher, K. M.; Geerke, D. P.; Malde, A. K.; Mark, A. E.; *J. Chem. Theory Comput.* **2018**, *14*, 5834. [Crossref]
140. Schindler, C. E. M.; Baumann, H.; Blum, A.; Böse, D.; Buchstaller, H.-P.; Burgdorf, L.; Cappel, D.; Chekler, E.; Czodrowski, P.; Dorsch, D.; Eguida, M. K. I.; Follows, B.; Fuchß, T.; Grädler, U.; Gunera, J.; Johnson, T.; Jorand Lebrun, C.; Karra, S.; Klein, M.; Knehans, T.; Koetzner, L.; Krier, M.; Leiendecker, M.; Leuthner, B.; Li, L.; Mochalkin, I.; Musil, D.; Neagu, C.; Rippmann, F.; Schiemann, K.; Schulz, R.; Steinbrecher, T.; Tanzer, E.-M.; Unzue Lopez, A.; Viacava Follis, A.; Wegener, A.; Kuhn, D.; *J. Chem. Inf. Model.* **2020**, *60*, 5457. [Crossref]
141. Gapsys, V.; Pérez-Benito, L.; Aldeghi, M.; Seeliger, D.; van Vlijmen, H.; Tresadern, G.; de Groot, B. L.; *Chem. Sci.* **2020**, *11*, 1140. [Crossref]
142. Shivakumar, D.; Harder, E.; Damm, W.; Friesner, R. A.; Sherman, W.; *J. Chem. Theory Comput.* **2012**, *8*, 2553. [Crossref]
143. Kuhn, B.; Gerber, P.; Schulz-Gasch, T.; Stahl, M.; *J. Med. Chem.* **2005**, *48*, 4040. [Crossref]
144. Gracia Carmona, O.; Gillhofer, M.; Tomasiak, L.; De Ruiter, A.; Oostenbrink, C.; *J. Chem. Theory Comput.* **2023**, *19*, 3379. [Crossref]
145. de Paula, F. T.; Frauches, P. Q.; Pedebos, C.; Berger, M.; Gnoatto, S. C. B.; Gossmann, G.; Verli, H.; Guimarães, J. A.; Graebin, C. S.; *Chem. Biol. Drug Des.* **2013**, *82*, 756. [Crossref]
146. Iida, S.; Kameda, T.; *J. Chem. Inf. Model.* **2023**, *63*, 3369. [Crossref]
147. Mollica, L.; Decherchi, S.; Zia, S. R.; Gaspari, R.; Cavalli, A.; Rocchia, W.; *Sci. Rep.* **2015**, *5*, 11539. [Crossref]
148. Wong, C. F.; *Expert Opin. Drug Discovery* **2023**, *18*, 1333. [Crossref]
149. Leysen, J. E.; Gommeren, W.; *Drug Dev. Res.* **1986**, *8*, 119. [Crossref]
150. Lee, K. S. S.; Yang, J.; Niu, J.; Ng, C. J.; Wagner, K. M.; Dong, H.; Kodani, S. D.; Wan, D.; Morisseau, C.; Hammock, B. D.; *ACS Cent. Sci.* **2019**, *5*, 1614. [Crossref]
151. Ziada, S.; Diharce, J.; Raimbaud, E.; Aci-Sèche, S.; Ducrot, P.; Bonnet, P.; *J. Chem. Inf. Model.* **2022**, *62*, 5536. [Crossref]
152. Guo, D.; Hillger, J. M.; IJzerman, A. P.; Heitman, L. H.; *Med. Res. Rev.* **2014**, *34*, 856. [Crossref]
153. Sykes, D. A.; Parry, C.; Reilly, J.; Wright, P.; Fairhurst, R. A.; Charlton, S. J.; *Mol. Pharmacol.* **2014**, *85*, 608. [Crossref]
154. Sherborne, B.; Shanmugasundaram, V.; Cheng, A. C.; Christ, C. D.; DesJarlais, R. L.; Duca, J. S.; Lewis, R. A.; Loughney, D. A.; Manas, E. S.; McGaughey, G. B.; Peishoff, C. E.; van Vlijmen, H.; *J. Comput. Aided Mol. Des.* **2016**, *30*, 1139. [Crossref]

Submitted: December 19, 2023
Published online: July 11, 2024